How the Surface Nanostructure of Polyethylene Affects Protein Assembly and Orientation

Thomas F. Keller,[†] Jörg Schönfelder,[†,§] Jörg Reichert,[†,⊥] Nunzio Tuccitto,[‡] Antonino Licciardello,[‡] Grazia M. L. Messina,[‡] Giovanni Marletta,[‡] and Klaus D. Jandt[†,*]

[†]Institute of Materials Science & Technology (IMT), Chair in Materials Science, Friedrich-Schiller-University Jena, Löbdergraben 32, 07743 Jena, Germany and [‡]Laboratory for Molecular Surfaces and Nanotechnology (LAMSUN), Department of Chemical Sciences, University of Catania, viale A. Doria 6, 95125 Catania, Italy. [§] Present address: Centro de Investigaciones Biológicas, Spanish Research Council (CSIC), Madrid, Spain. [⊥] Present address: SurA Chemicals GmbH, Am Pösener Weg 2, 07751 Bucha, Germany.

ABSTRACT Protein adsorption plays a key role in the biological response to implants. We report how nanoscale topography, chemistry, crystallinity, and molecular chain anisotropy of ultrahigh molecular weight polyethylene (UHMWPE) surfaces affect the protein assembly and induce lateral orientational order. We applied ultraflat, melt drawn UHMWPE films to show that highly oriented nanocrystalline lamellae influence the conformation and aggregation into network structures of human plasma fibrinogen by atomic force microscopy with unprecedented clarity and molecular resolution. We observed a transition from random protein orientation at low concentrations to an assembly guided by the UHMWPE surface nanotopography at a close to full surface coverage on hydrophobic melt drawn UHMWPE. This assembly differs from the arrangement at a hydrophobic, on the nanoscale smooth UHMWPE reference. On plasma-modified, hydrophilic melt drawn UHMWPE surfaces that retained their original nanotopography, the influence of the nanoscale surface pattern on the protein adsorption is lost. A model based on protein–surface and protein–protein interactions is proposed. We suggest these nanostructured polymer films to be versatile model surfaces to provide unique information on protein interactions with nanoscale building blocks of implants, such as nanocrystalline UHMWPE lamellae. The current study contributes to the understanding of molecular processes at polymer biointerfaces and may support their future design and molecular scale tailoring.

KEYWORDS: surface nanostructure · ultrahigh molecular weight polyethylene (UHMWPE) · fibrinogen · biointerface · protein–surface interaction · molecular design of implant

The nanostructure of implant surfaces is more and more recognized to strongly influence the protein adsorption and the subsequent cellular response.[1,2] This stresses the significance of the local protein assembly for the biocompatibility and functionality of biomaterials. It demands a profound understanding and capability to control protein–surface interactions, particularly for the growing number of polymeric biomaterials.[3]

One well-known polymeric biomaterial with specific functional requirements, such as impact strength, abrasion resistance, and low friction, is ultrahigh molecular weight polyethylene (UHMWPE). Its main application in the biomedical field is in total hip or knee endoprosthesis (TEP) where it slides against a ceramic[4] or metallic[5] bearing partner. One of the major lifetime limiting factors of such TEPs is the UHMWPE wear and friction behavior. UHMWPE wear debris in the surrounding synovial fluid may activate inflammation reactions and cause osteolysis and mechanical aseptic loosening of the implant.[6]

Recently, it was reported that protein layers adsorbed from the synovial fluid onto the UHMWPE surface can reduce the wear rate depending on the type, amount, and conformation of the adsorbed proteins.[7,8] Protein and more general biomolecule layers are largely influenced by the biomaterials' surface characteristics, such as surface topography,[1,2,9,10] surface chemistry,[7,11] and surface crystallinity,[12] but also surface anisotropy on the molecular and supramolecular scale.[13]

Introducing molecular chain orientation in UHMWPE by uniaxial compression or stretching can enhance the wear resistance as compared to the unoriented UHMWPE in water[14] and in the dry state.[15] With bovine serum albumin as lubricant, however, the improvement of wear resistance diminishes.[16] This indicates the crucial role of the boundary layer between the UHMWPE surface and the wear counterpart mediated by the lubricating synovial liquid and the adsorbed protein layer.

It is not clear how the UHMWPE surface topography and surface chemistry, and more specifically the two basic building blocks of the semicrystalline UHMWPE (*i.e.*, the crystalline chain fold lamellae and the surrounding amorphous regions) influence the protein adsorption. It is, therefore, an

* Address correspondence to k.jandt@uni-jena.de.

Received for review January 21, 2011 and accepted March 1, 2011.

Published online March 18, 2011
10.1021/nn200267c

important and timely question to obtain a deeper insight into protein adsorption processes on nanometer-scale structured polyethylene surfaces.

The rough surface of a clinical UHMWPE implant impedes high spatial resolution of surface-sensitive techniques, such as atomic force microscopy (AFM) that permits the resolution of single proteins.[17] So far, AFM analysis on such rough, similar polymeric implant surfaces, such as low density polyethylene (LD-PE) or polydimethylsiloxane (PDMS), did not yield detailed information on the protein arrangement and conformation.[18]

Previously, we reported the first time creation of ultraflat, highly oriented UHMWPE films by a melt drawing (MD) technique.[19] During the MD process, a highly oriented and nanostructured surface develops on the MD UHMWPE films by strain-induced, crystallization-driven self-assembly.[20−23] The surface morphology of MD UHMWPE films consists of highly regular, stacked nanocrystalline lamellae of high orientation that are interconnected by amorphous interlayers.[19]

For the protein adsorption in the present work, human plasma fibrinogen (HPF) was chosen, as it is intrinsically anisotropic, amphiphilic, and relevant for current applications of UHMWPE and further polymeric implant materials, such as polyethylene terephthalate (PET)[24] or poly(lactide)-based homo- or copolymers.[25] Although HPF is rarely found in the human synovial fluid of an intact healthy joint,[26] HPF concentrations of 0.15−2.10 g/L have been observed in the case of osteoarthritis.[27] In most inflamed joints, the coagulation system is activated, leading to a local generation of fibrin.[28]

Here, we report for the first time to the best of our knowledge the concentration-dependent assembly and orientation of HPF on hydrophobic and plasma-treated hydrophilic nanostructured UHMWPE surfaces. We discuss the influence of the UHMWPE biomaterials' surface topography, surface chemistry, as well as crystallinity and molecular chain anisotropy on the conformation and aggregation into network structures of adsorbed HPF based on AFM analysis. We further deduce information on protein−surface and protein−protein interactions obtained from concentration-dependent adsorption experiments.

In this framework, the orientation state of proteins adsorbed on the surface of MD UHMWPE films is of special interest, as the latter determines the surface functionality and lubrication properties. The control of protein adsorption by the biomaterials' nanostructure is one key in bionanotechnology for the future design of implant surfaces in contact with body fluids, such as TEPs, devices in the vascular field, or biosensors.

RESULTS

Native and Plasma-Treated MD UHMWPE Surfaces. Ultraflat UHMWPE films were drawn after evaporation of the solvent[19,20] from the UHMWPE melt located on a glass slide on top of a heating plate, as sketched in Figure 1. Melt drawing of the semicrystalline UHMWPE induces a crystallographic fiber texture that consists of highly oriented crystalline chain fold lamellae interconnected by amorphous interlayers.[19] The polymer chains are oriented parallel to the crystallographic *c*-direction of the orthorhombic crystal system of UHMWPE (*i.e.*, along [001]), which coincides with the melt drawing direction.[29]

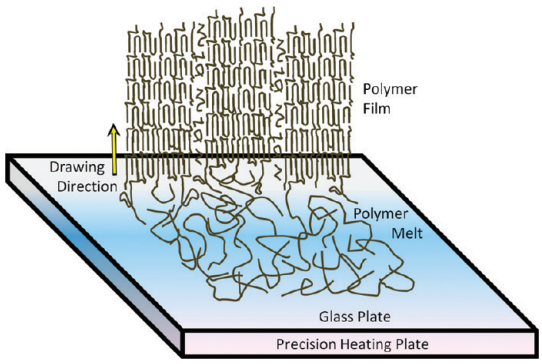

Figure 1. Sketch of the melt drawing technique used to prepare MD UHMWPE films.[19,20] The free-standing UHMWPE film was drawn from the polymer melt on a glass plate on top of a heating plate and subsequently fixed on a glass slide.

AFM. AFM micrographs of the surface morphology of ultraflat native and argon plasma-treated MD UHMWPE surfaces are shown in Figure 2a,b, respectively. The MD UHMWPE surfaces are anisotropic and exhibit a regular pattern of nanoscale lamellae packed into neighboring stacks, as sketched in Figure 2, indicating the lamellar orientation with their thickness parallel to the film drawing direction. The crystallographic fiber texture implies that the crystalline surface planes of the stacked lamellae are {*hk*0} planes.[29] Ultraflat means here sufficiently flat to resolve single adsorbed proteins, that is, surfaces with a typical root-mean-square roughness (rms) of 2 ± 0.5 nm on an area of 500 nm × 500 nm.[19]

A cross-section view of the macromolecular assembly of a MD UHMWPE film with typical dimensions relevant for the present study is schematically shown in Figure 3a. The lamellae are embedded in the amorphous matrix of interconnecting tie molecules edge-on with respect to the film surface. The mean lamellar length and thickness were deduced from Figure 2 to be 95 ± 12 and 24 ± 8 nm, respectively. Within a single stack, lamellae protrude 3 ± 2 nm out of the amorphous interlayers. Amorphous regions between neighboring stacks of lamellae are 38 ± 10 nm wide and 4 ± 1 nm high. Figure 3b schematically shows the typical trinodular conformation of HPF. It is amphiphilic and consists of two hydrophobic polypeptide D domains connected to a centered hydrophobic E domain. Attached to each D domain is an outer positively charged hydrophilic αC domain.[30]

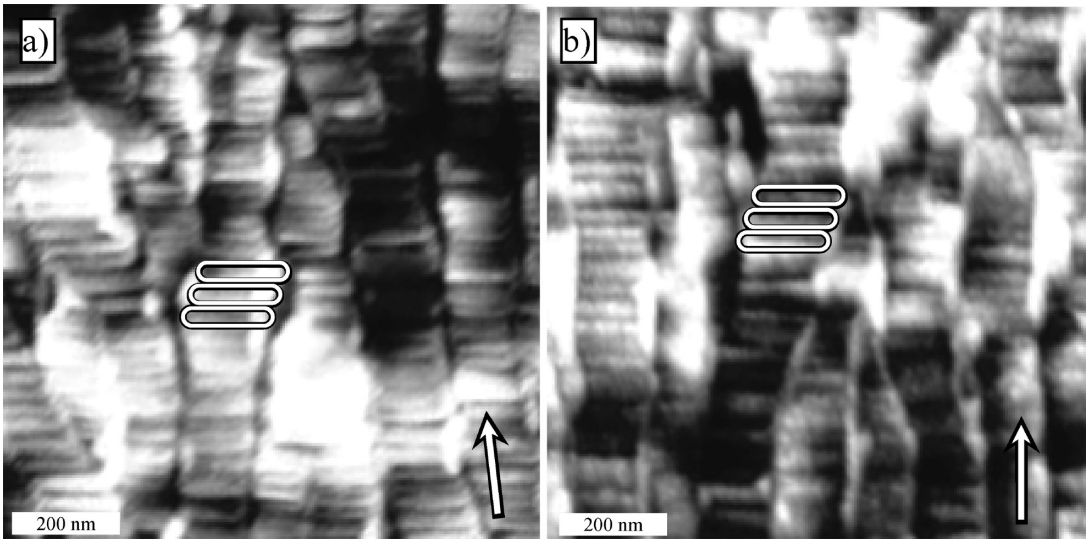

Figure 2. AFM topographic image of (a) the native MD UHMWPE surface and (b) after plasma modification. Image sizes are 1 μm $\times$ 1 μm. The gray scale from black to white corresponds to a height difference of 20 nm. The arrows indicate the drawing direction. As a guide to the eye, three stacked crystalline chain fold lamellae are schematically encircled in each image.

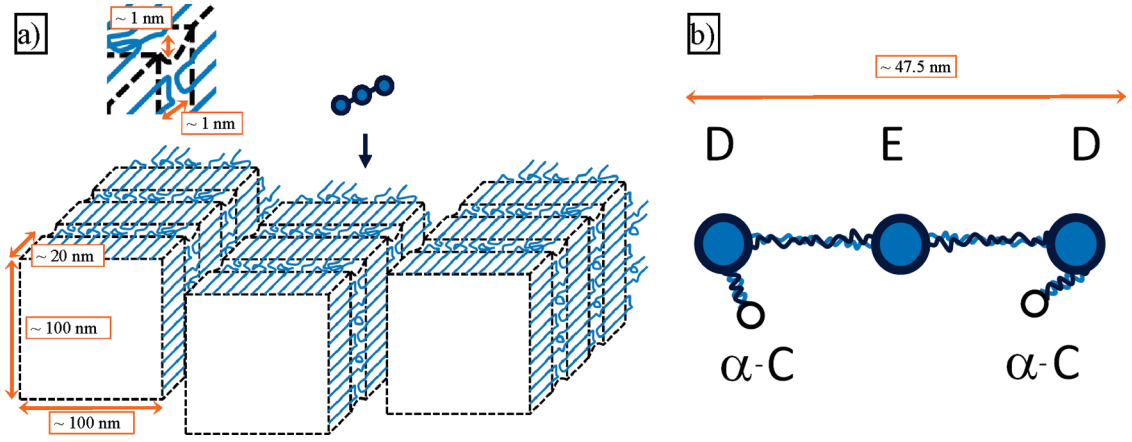

Figure 3. (a) Sketch of the UHMWPE film morphology in the bulk and on the surface (upper side of sketch).[19] A HPF molecule is added to the sketch to animate the adsorption of HPF onto such MD UHMWPE surfaces. The inset on the top is a magnification of the edge between crystalline lamellae and the amorphous region. Dashed lines are a guide to the eye. b) Sketch of a single HPF molecule with its typical trinodular shape and the hydrophobic centered E and D and hydrophilic αC domains.[30,36]

ToF-SIMS, XPS, and Contact Angle Analysis. The spectra in Figure 4a,b show time-of-flight secondary-ion mass spectrometry (ToF-SIMS) intensities of molecule fragments as a function of atomic mass from the hydrophobic and plasma-treated hydrophilic UHMWPE film surface, respectively. From that, it is clear that the hydrophilicity introduced by the plasma treatment originates from polar oxygen groups present on the plasma-treated hydrophilic surface (Figure 4b) which are absent on the hydrophobic surface (Figure 4a). Similarly, high-resolution X-ray photoelectron spectroscopy (XPS) spectra of the untreated MD UHMWPE surface in the vicinity of the C1s binding energy confirm the sole presence of the C−C bond at 284.7 eV (Figure 4c) and the introduction of different polar oxygen groups like C−O bonds at 286.5 eV, C═O bonds at 288.0 eV, and O−C═O bonds at 289.2 eV[31] on the plasma-treated hydrophilic MD UHMWPE surface (Figure 4d).

Static contact angles were determined to be 104 $\pm$ 3° for the hydrophobic MD UHMWPE film, whereas the plasma-modified hydrophilic UHMWPE surface exhibited a contact angle of 54 $\pm$ 3°. Therefore, both the hydrophobic and hydrophilic regimes were covered, as the transition between a low and a high adhesion force between fibrinogen and a low density polyethylene (LDPE) surface was reported to be in the water contact angle range of 60−65°.[32]

It is important to note that a significant decrease in water contact angle was induced without any observable alteration of the surface morphology by carefully adjusting the duration of plasma treatment and chamber

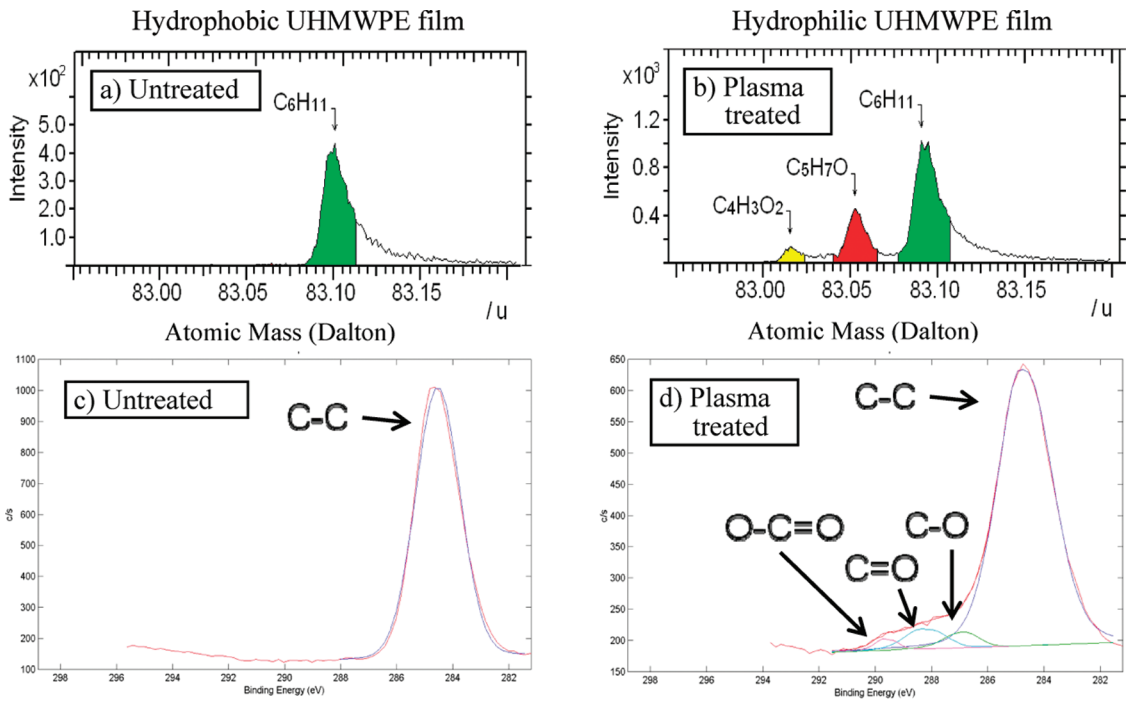

Figure 4. Time-of-flight secondary-ion mass spectrometry (ToF-SIMS) of the UHMWPE films (a) prior to and (b) after plasma treatment. XPS high-resolution spectra of the C1s peak of the UHMWPE films (c) prior to and (d) after plasma treatment.

pressure, as the AFM images of the native hydrophobic and plasma-treated hydrophilic UHMWPE films in Figure 2a,b confirm. The somewhat coarser image of the plasma-treated surface indicates a stronger tip-surface interaction as compared to the hydrophobic surface.

HPF Assembly on Nanostructured Hydrophobic MD UHMWPE Surfaces. HPF was allowed to adsorb on hydrophobic MD UHMWPE surfaces from different concentrations in phosphate buffered saline solution (PBS). As a reference, Figure 5a shows the native hydrophobic MD UHMWPE surface prior to adsorption with a zoom of three stacked neighboring chain fold lamellae magnified and sketched on the right. Figure 5b–e shows AFM height images of a series of hydrophobic MD UHMWPE surfaces, on which HPF was adsorbed from PBS solutions at a HPF concentration of 1 mg/L (Figure 5b), 5 mg/L (Figure 5c), 8 mg/L (Figure 5d), and 10 mg/L (Figure 5e). For any of the applied HPF concentrations, the lamellar morphology of the underlying MD UHMWPE surface can be distinguished. Apart from the native MD UHMWPE surface morphology shown in Figure 5a, any further structural features were assigned to HPF in typical states of assemblies and conformations, that is, single molecules of HPF, aggregates, or network structures.

HPF Assembly on Hydrophobic, on the Nanoscale Smooth MD UHMWPE Surfaces. Figure 6a is an AFM micrograph of an ultraflat, hydrophobic MD UHMWPE surface that exhibits large, ~250 nm thick and ~100 nm wide, characteristics on the nanoscale smooth UHMWPE regions. The origin of these regions is not yet understood but assigned to either extended lamellae or an amorphous overlayer. The overall lamellar structure visible in Figure 6a assures that the surface indeed is UHMWPE, as the glass surface beneath does not consist of lamellae (image not shown).

AFM micrographs of the polymer film after adsorption of HPF from concentrations of 1 and 10 mg/L are shown in Figure 6b,c and Figure 6d, respectively. In the framework of the present investigation, it is worth noting that the formation of a star-like HPF arrangement is observed at hydrophobic, on the nanoscale smooth UHMWPE surfaces at a low concentration of 1 mg/L (Figure 6c,e). At a high concentration of 10 mg/L (Figure 6d,f), HPF molecules form a ringlike network structure without any observable surface-induced orientation.

Influence of Surface Chemistry on HPF Adsorption on Nanostructured MD UHMWPE Surfaces. Figure 7a shows a topographic AFM image of a plasma-treated, hydrophilic MD UHMWPE surface prior to adsorption with a magnification of three stacked neighboring chain fold lamellae and a sketch on the right similar to the hydrophobic surface in Figure 5a. Figure 7b,c shows AFM micrographs of the hydrophilic MD UHMWPE surface with adsorbed HPF from PBS buffer solution of 5 and 10 mg/L concentration, respectively. The adsorption conditions were the same as for the hydrophobic surfaces.

DISCUSSION

HPF Assembly and Orientation on Native Hydrophobic, Nanostructured MD UHMWPE Surfaces. Figure 5a–e shows

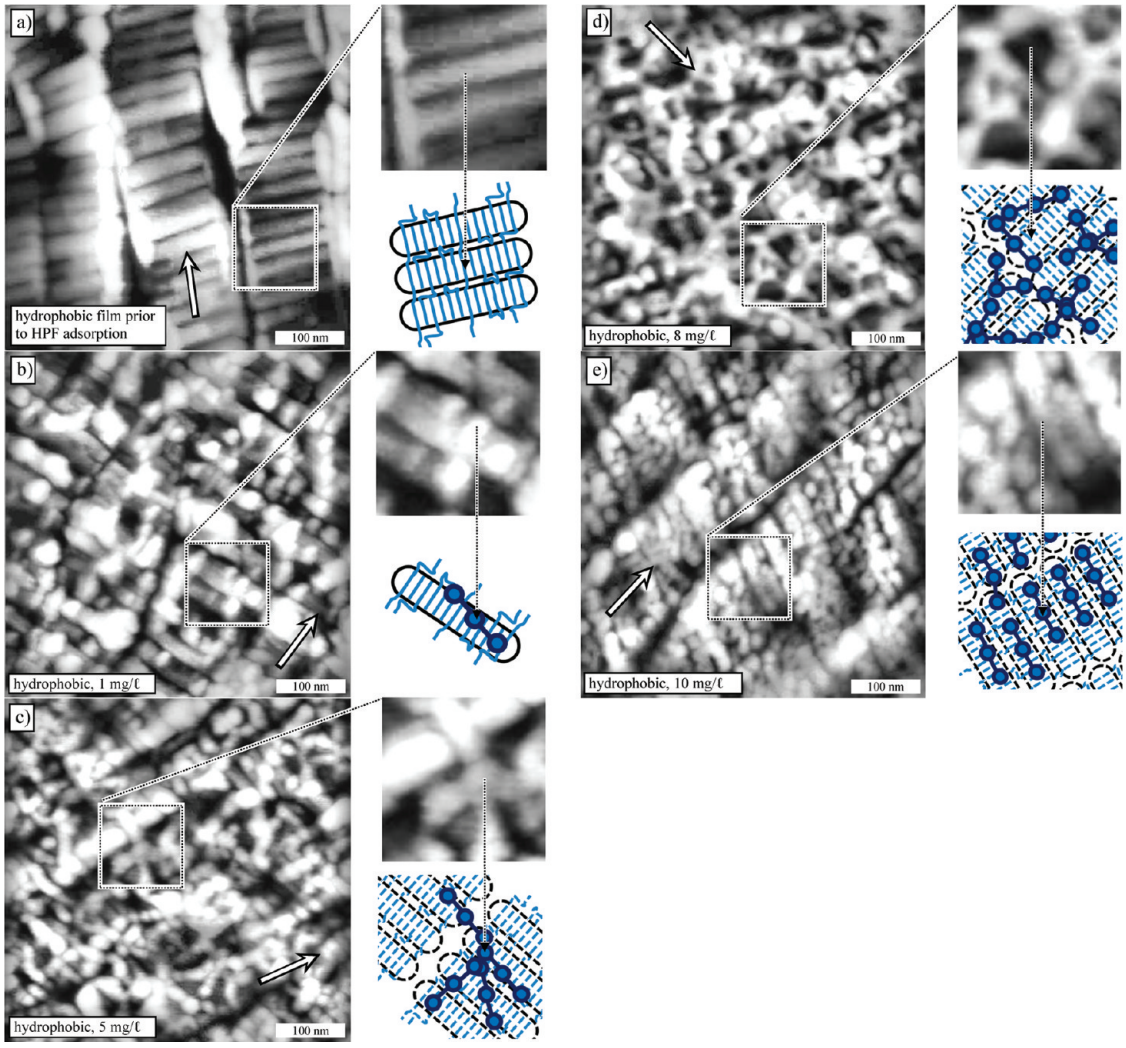

Figure 5. (a−e) Topographic AFM images of hydrophobic MD UHMWPE surfaces, on which HPF was adsorbed from PBS buffer solution at different concentrations. The image sizes are 500 nm × 500 nm; the gray scale from black to white corresponds to a height difference of 20 nm. Arrows indicate the drawing direction. Magnifications of selected regions with typical features are sketched to the right of the panels. (a) Native nanostructured MD UHMWPE surface. (b−e) Nanostructured MD UHMWPE surfaces with HPF adsorbed from concentrations of (b) 1 mg/L, (c) 5 mg/L, (d) 8 mg/L, and (e) 10 mg/L. Dashed lines in the sketch indicate that the adsorbed HPF does not allow seeing the underlying UHMWPE lamellar structure.

AFM topographic images of hydrophobic, nanostructured MD UHMWPE surfaces, on which HPF was adsorbed from PBS buffer solution at different concentrations. As reference, it serves as the native ultraflat UHMWPE film surface in Figure 5a. Figure 5b is an AFM micrograph of the native hydrophobic MD UHMWPE surface after the adsorption of HPF from a concentration of 1 mg/L. Isolated HPF molecules are identified by their trinodular structure and conformation, such as can be seen on the right of Figure 5b. This shows that on semicrystalline thermoplastic polymer surfaces, molecular resolution of single HPF proteins can be achieved by AFM, provided the surface is sufficiently flat or regular. Mean length, width, and thickness of the adsorbate are 54.0 ± 4.0 nm, 16.0 ± 3.0 nm, and 1.4 ± 0.4 nm, respectively, and given in Table 1. Therefore, the mean length is within the range of 45−60 nm, that is, the conformation-dependent length of a single HPF molecule at a surface.[33,34]

At a low concentration (1 mg/L, Figure 5b), the observation of isolated HPF molecules in typical trinodular conformations agrees with reports of the adsorption on highly ordered pyrolytic graphite (HOPG).[35] On hydrophobic HOPG, HPF adsorbs at low concentration mostly as single flat-on, rod-like molecules and indicates that the adsorption is dominated by the hydrophobic−hydrophobic interaction between the hydrophobic HPF D or E domains and the hydrophobic surface and induces the trinodular molecular appearance.[35]

At intermediate concentrations, connections between adjacent HPF molecules (5 mg/L, Figure 5c) and the onset and formation of ringlike network structures around centered protein free voids (8 mg/L, Figure 5d) consisting of several HPF molecules

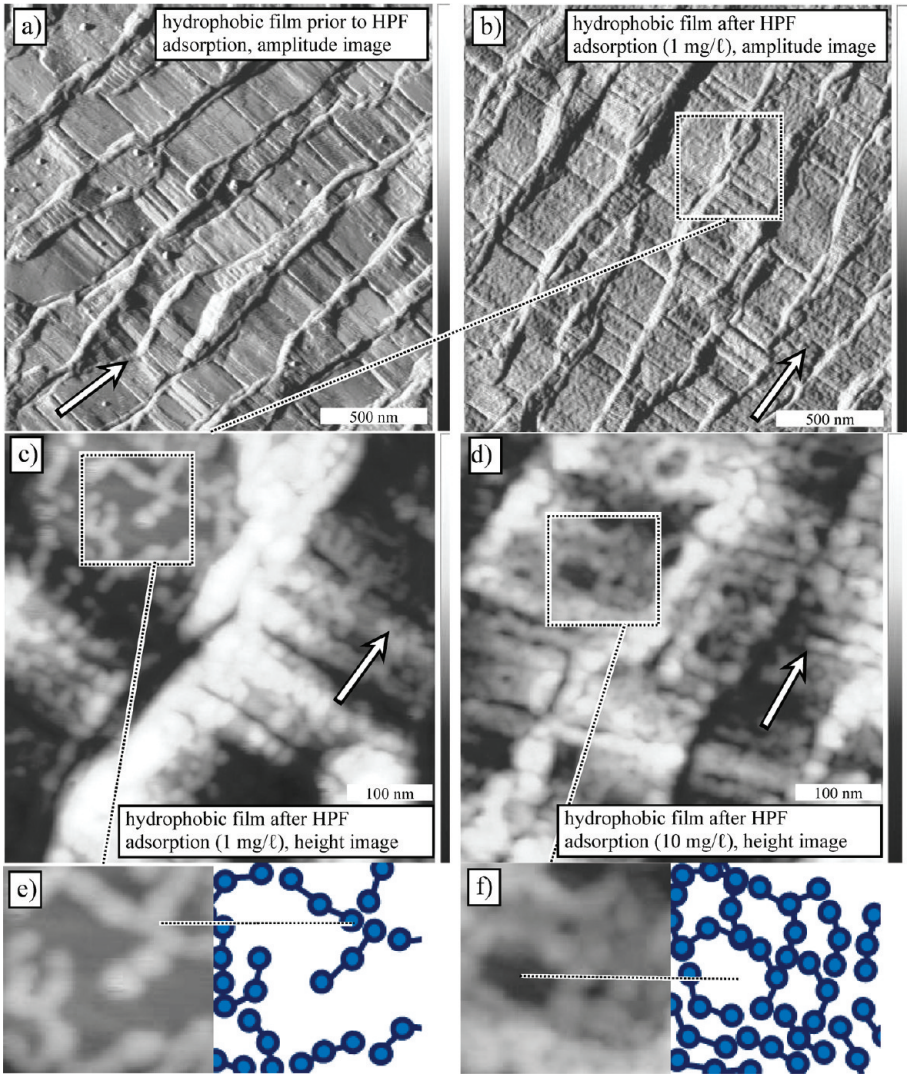

Figure 6. AFM images of hydrophobic, on the nanoscale smooth MD UHMWPE surfaces. Amplitude image (a) prior to and (b) after protein adsorption from PBS buffer (concentration 1 mg/L). The image size is 2 μm $\times$ 2 μm. The gray scale on the right corresponds to an amplitude difference of 250 mV for both images. (c) High-resolution height image of the framed area in panel b. (d) High-resolution height image of a similar area after adsorption from PBS buffer with a concentration of 10 mg/L. The image sizes in (c) and (d) are 500 nm $\times$ 500 nm, and the gray scale on the right corresponds to a height difference of 20 nm. Arrows indicate the drawing direction. Panels e and f show the magnification of panels c and d along with a corresponding sketch.

indicate the increased influence of protein−protein interactions.[30] The mean length and width of proteins are 53.0 $\pm$ 3.4 and 19.6 $\pm$ 1.2 nm and, therefore, close to the dimensions of HPF observed at lower concentrations (Table 1), whereas the average thickness increases due to a significant overlap within the ringlike structure visible in the high-resolution topographic image on the right side of Figure 5d.

The ringlike network structures show that an increasing protein concentration facilitates protein−protein interactions due to an increased protein density on the surface. The HPF intermolecular mean distance is reduced, which enables short-range protein−protein forces to induce protein rearrangements, such as into network structures. Aggregations or network structures are therefore a signature of both a sufficiently high protein concentration and protein−protein interactions that dominate the still present protein−surface interactions.

Protein−protein interactions may induce various HPF assemblies and impede a homogeneous surface coverage since approaching proteins are incorporated into the network of adjacent, already adsorbed proteins. These protein−protein interactions can be subdivided into first a lateral side-to-side and second an end-to-end protein−protein interaction. The first interaction connects the hydrophobic D or E domains of adjacent HPF molecules (perpendicular to elongated fibrinogen molecules) and forms a dense aggregation.[36] The second interacts between one end of an individual fibrinogen molecule and another end of a second molecule *via* their hydrophilic αC domains.[37]

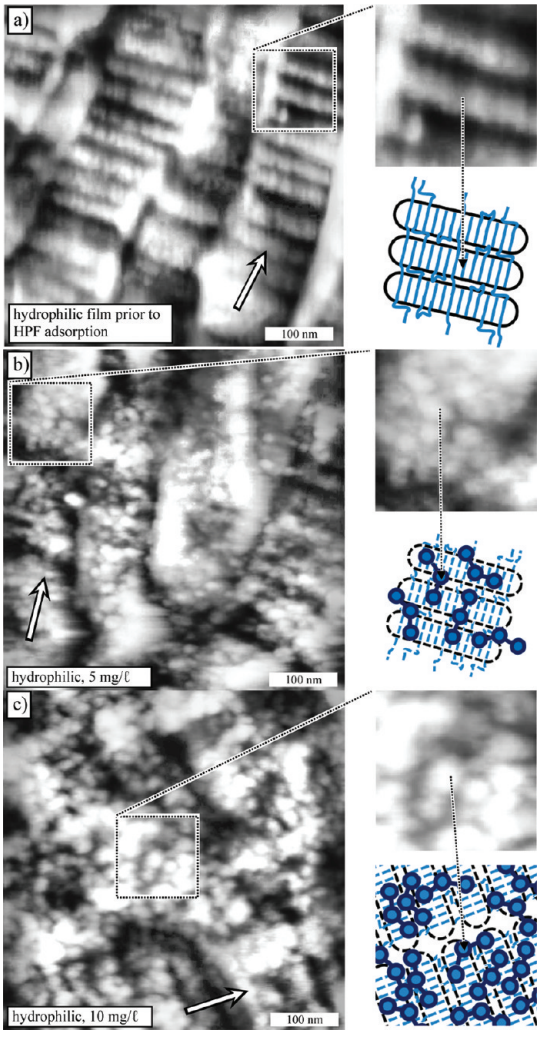

Figure 7. Left: AFM topographic height images of nanostructured, plasma-modified hydrophilic MD UHMWPE surfaces, on which HPF was adsorbed from PBS buffer solution at different concentrations. The image sizes are 500 nm × 500 nm, and the gray scale from black to white corresponds to a height difference of 20 nm. Arrows indicate the drawing direction. Right: Magnifications of selected regions along with sketch of the arrangement of adsorbed HPF onto the hydrophilic UHMWPE surface. (a) After plasma modification, (b,c) after adsorption of HPF from a concentration of (b) 5 mg/L and (c) 10 mg/L. Dashed lines in the sketch indicate that the adsorbed HPF does not allow seeing the underlying UHMWPE lamellar structure.

HPF molecules attached to each other on one end with the opposite D or αC domains spreading across crystalline and amorphous regions of the native MD UHMWPE surface, such as observed in Figure 5c, are a signature of dominating end-to-end interactions by the outer αC domains.[30] Further, partial or complete ringlike network structures around centered voids, such as at a concentration of 8 mg/L magnified and sketched on the right of Figure 5d, indicate end-to-end protein−protein interactions and suggest an aggregation mechanism *via* the outer hydrophilic αC domains, leading to a surface coverage with homogeneously distributed HPF ringlike network structures. Such ringlike networks comprising voids with protein free areas inside are the favorable lateral HPF arrangement on hydrophobic HOPG surfaces persisting up to high concentrations of 50 mg/L, that is, far in the regime of multiple HPF layers.[35]

These up to now described characteristics of the assembly of HPF on native hydrophobic MD UHMWPE surfaces as deduced from Figure 5b−e closely resemble the adsorption on hydrophobic surfaces governed by surface chemistry.

Furthermore, at a low concentration (1 mg/L, Figure 5b), there is a tendency for a preferred orientation along the underlying native MD UHMWPE surface, that is, one axis of the HPF molecule directs either parallel or perpendicular to the lamellae width, as can be seen on the right along with the corresponding sketch. In this case, the axis of a single HPF molecule is oriented close to parallel to the lamellar width direction. The reasons for the behavior are two-fold: on the molecular scale, the orientation of the HPF axis may be influenced by the UHMWPE crystal structure, and second, on the supramolecular nanoscale, an orientation of HPF may be induced by the surface topography with lamellar dimensions similar to the size of the HPF molecules.

Similarly, at intermediate concentrations of 5−8 mg/L, still in the regime of submonolayer coverage as seen from Figure 5c,d, we observed nonrandom, oriented HPF molecules. They are involved in the HPF network and tend to align in either parallel or perpendicular orientation with respect to the drawing direction. The shape of a HPF ringlike network therefore appears noncircular. Such noncircular, edged ringlike networks with protein-free, centered voids indicate that the overall orientation of the network is affected by the UHMWPE lamellar arrangement and surface topography. Two or more HPF molecules partially form interlamellar bridges across amorphous regions. Several ring diameters of the ringlike network structures are clearly visible at a concentration of 8 mg/L, varying from two up to six participating HPF molecules.

At a high HPF buffer concentration of 10 mg/L (Figure 5e), the native hydrophobic MD UHMWPE surface is uniformly covered with adsorbed proteins at a close to monolayer coverage. The close-up in Figure 5e on the right shows HPF molecules in trinodular shape adsorbed on single lamellae incorporated in the densely packed protein film. Single proteins cannot be clearly separated, and therefore, lateral dimensions cannot be determined precisely. We observed a surprisingly clear assembly of the protein layer resembling the underlying native MD UHMWPE surface morphology with its typical topography. HPF ringlike network structures are still present, although with a significantly reduced diameter and without the centered void.

Whereas on hydrophobic HOPG ring network structures are known to dominate beyond concentrations of 10 mg/L,[35] Figure 5e suggests that the latter is

TABLE 1. Concentration-Dependent HPF Arrangement and Dimensions of Adsorbed HPF Molecules on Hydrophobic and Hydrophilic UHMWPE Surfaces: Standard Deviations Were Obtained from at Least 10 Independent Measurements ($n \geq 10$)

HPF concentration	HPF arrangement	length (nm)	width (nm)	height (nm)
1 mg/L hydrophobic	single proteins	54.0 ± 4.0	16.0 ± 3.0	1.4 ± 0.4
5 mg/L hydrophobic	onset of protein networks	52.1 ± 3.3	17.8 ± 2.4	2.7 ± 0.9
8 mg/L hydrophobic	protein network	53.0 ± 3.4	19.6 ± 1.2	~4−8
10 mg/L hydrophobic	densely packed protein layer	na	na	~4−6
5 mg/L hydrophilic	randomly packed protein layer	46.3 ± 2.6	14.0 ± 1.5	2.6 ± 0.3
10 mg/L hydrophilic	randomly packed dense protein layer	na	na	na

significantly suppressed or hindered on the hydrophobic MD UHMWPE surface. We hypothesize that the observed tightly packed molecular assembly of HPF onto the crystalline UHMWPE lamellae is not solely due to a "dense packing effect" at a close to monolayer coverage. Rather, we regard the interplay of end-to-end protein−protein and protein−surface interactions as relevant forces to facilitate the adsorption on favored adsorption sites, such as single lamellae in favor of overlapping lamellae stacks.

A favored adsorption has been observed at atomic steps of HOPG and related to a locally increased surface free energy.[35,36] This indicates that surface topographic features, such as geometrical as well as energetic aspects, influence the arrangement of protein layers formed during adsorption for any specific implant-surface/protein combination. We recently reported that α-helical poly(L-lysine) (α-PLL) polypeptide chains can be templated on MD high-density polyethylene surfaces.[13] In this work, we suggested that the alignment of the layer-by-layer adsorbed α-PLL is induced thermodynamically by a surface free energy minimization on a molecular or supramolecular scale. On the molecular scale, this could be a geometric accommodation of the ~1 nm diameter thick α-PLL rods into the local surface potential of two neighboring PE chains along the [010] direction of a PE lamellar crystal surface. On the supramolecular scale, the nanotopography generated by ridges or ledges between crystalline PE lamellae and the amorphous regions could induce the orientation of the polypeptide.[13]

In the current work, the homogeneous coverage of the crystalline lamellae with HPF in Figure 5e suggests that the driving force for the favored HPF assembly onto the crystalline lamellae is due to a local increase in surface free energy on the crystalline sites as compared to the amorphous region. The crystalline lamellae exhibit a higher surface free energy than the amorphous regions, leading to an increased wettability and hydrophilicity, which may in turn enhance the adsorption of proteins.[38] This difference in surface free energy between the two building blocks could trigger a locally higher affinity of HPF to the more hydrophilic crystalline sites of the native MD UHMWPE. Further, it has to be noted that, at high concentrations, a multistage adsorption process becomes likely,[39] which permits rearrangements and may facilitate the here observed high degree of regularity. Such rearrangements could include a totally smaller amount of ringlike networks, smaller diameters of the rings, and the partial orientation of HPF molecules along the crystalline lamellae.

HPF Assembly and Orientation on Hydrophobic, on the Nanoscale Smooth MD UHMWPE Surfaces. Figure 6 enlightens the influence of the crystalline/amorphous nanotopography on the HPF arrangement on the native hydrophobic, nanostructured MD UHMWPE. It shows the HPF assembly on a UHMWPE surface, which is smooth on the nanoscale. The visible lamellar structure typical for crystalline lamellae clearly identifies the UHMWPE surface and distinguishes it from the underlying glass substrate. At a low concentration of 1 mg/L (Figure 6c, e) a star-like arrangement of HPF molecules is observed. Such star-like arrangements have been observed at similar low concentrations on HOPG on areas sufficiently far from atomic steps.[35] As on both HOPG and the smooth MD UHMWPE surface protein guiding topographic features are absent, we assume the star-like HPF arrangement to be of general nature for the adsorption at low concentration on hydrophobic surfaces, which are smooth on the nanoscale. The appearance of protein−protein interactions at low concentrations indicates an enhanced surface diffusion of single HPF molecules on surfaces which are smooth on the nanoscale. An enhanced surface diffusion on the hydrophobic, on the nanoscale smooth MD UHMWPE surface could be facilitated by a locally reduced surface roughness. The latter becomes obvious by comparing representative line profiles of MD UHMWPE surfaces which are nanostructured and smooth on the nanoscale, as shown in Figure 8.

The absence of topographic features facilitates end-to-end protein−protein interactions to dominate the HPF assembly.

At a high concentration of 10 mg/L (Figure 6d,f), on the hydrophobic, on the nanoscale smooth MD UHMWPE surface, the HPF arrangement consists of a homogeneous HPF ringlike network structure with essentially no favored, surface-induced orientation. Again, this agrees with observations on HOPG at similar concentrations.[35]

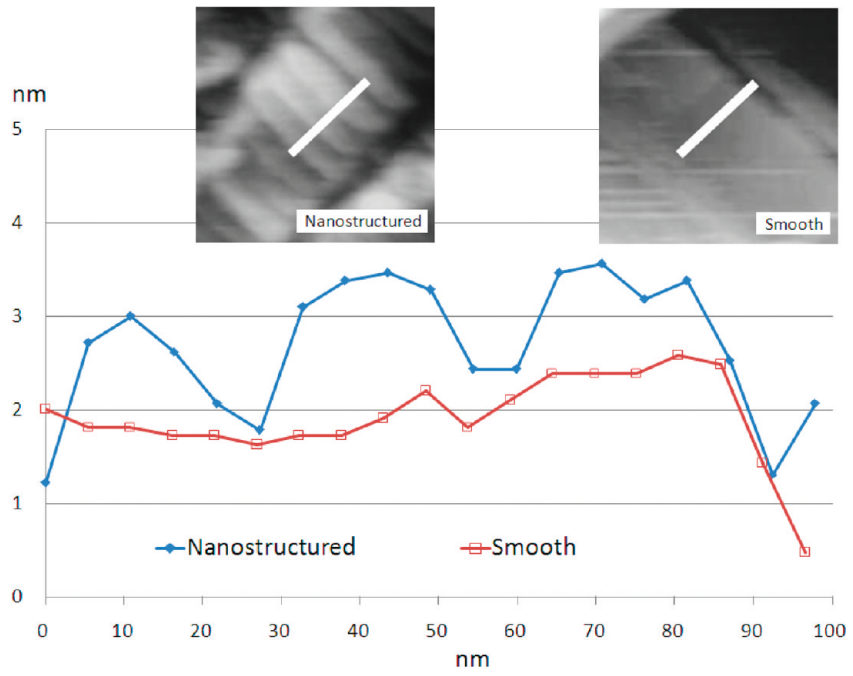

Figure 8. Representative line profiles of nanostructured and on the nanoscale smooth MD UHMWPE surfaces. The insets are magnifications of the corresponding AFM images, and the white bars indicate directions of the line profiles.

The comparison of the protein assembly on the hydrophobic, on the nanoscale smooth and the nanostructured MD UHMWPE surface suggests that the surface morphology of the latter suppresses the surface diffusion of single HPF molecules at low concentration and the natural aggregation into ringlike network structures at high concentration. Furthermore, at close to monolayer coverage, the nanostructured surface morphology suppresses the ringlike networks and confines the mean ring diameters of the ring networks to the lateral size of the stacked crystalline UHMWPE lamellae. This indicates that ringlike network and void formation is generic for HPF adsorption at sufficiently high concentrations on hydrophobic, smooth surfaces with a minimal lateral distance of features in the order of the diameter of the ringlike structures (like atomic steps of HOPG, lamellae size of UHMWPE, *etc.*). The HPF assembly on hydrophobic surfaces is therefore crucially dependent on the lateral distance of surface features and thus on the nanoscale surface morphology.

Influence of Surface Chemistry on HPF Assembly on Nanostructured MD UHMWPE Surfaces. Figure 7a–c shows the plasma-treated, hydrophilic MD UHMWPE surface prior to protein adsorption and the HPF assembly on the latter surface after adsorption from concentrations of 5 and 10 mg/L HPF in PBS, respectively. As can be seen in Figure 7b,c for both concentrations, the adsorption onto the hydrophilic MD UHMWPE surface is dominated by the random arrangement of individual HPF molecules in a globular conformation. At neither concentration, a systematic HPF orientation with respect to the underlying MD UHMWPE surface can be observed. Any signature of intermolecular protein–protein interactions, such as agglomeration of adjacent HPF molecules or protein ringlike networks, is entirely absent at concentrations of 5 and 10 mg/L on the nanostructured hydrophilic MD UHMWPE surface. This implies that the driving force for adsorbate–surface nucleation is greater than that for the formation of protein–protein interactions. Therefore, the adsorption mechanism is different from that on hydrophobic surfaces, for example, Figure 5c,e, where protein–protein interactions govern the final film structure.[30] Obviously, the reduction of the water contact angle of the MD UHMWPE surface from hydrophobic (*i.e.*, 104 ± 3°) to hydrophilic (*i.e.*, 54 ± 3°) was sufficient to cross the transition from a strong to a less strong adhesion force between the fibrinogen and the UHMWPE at a water contact angle of 60–65°.[32]

At a concentration of 5 mg/L, single HPF molecules adsorbed on the hydrophilic MD UHMWPE surface are determined to be 46.3 ± 2.6 nm long, 14.0 ± 1.5 nm wide, and 2.6 ± 0.3 nm thick (Table 1). Therefore, the lateral dimensions of single HPF molecules are reduced compared to the corresponding hydrophobic surface. The decreased lateral size of the HPF indicates a globular or shortened trinodular conformation with reduced unfolding as compared to the hydrophobic UHMWPE surface. In agreement with the model of HPF adsorption on hydrophilic mica[40] or silicon,[41] we assume the αC domains to be attached to the hydrophilic UHMWPE surface thus shielding the hydrophobic D and E domains which are piling up on top.[30] This permits a lower degree of surface-induced conformational changes and less denaturation[42] than on

the hydrophobic MD UHMWPE surface, where HPF shows its typical trinodular conformation. For a concentration of 10 mg/L, a dense layer of HPF molecules spreading on the hydrophilic MD UHMWPE surface impedes the determination of the mean size of individual HPF molecules.

The adsorption of proteins on surfaces is mainly due to electrostatic and van der Waals interactions. On hydrophobic surfaces, the protein adsorption is further driven by hydrophobic or entropic forces, as the total entropy is increased by removing water molecules from both the material surface and the protein surface back into the buffer solution. The conformation of proteins on an implant surface is, therefore, strongly dependent on the surface chemistry and the nature of the protein itself. For collagen, for example, it was found that while the adsorbed amount is only affected by the surface chemistry, the supramolecular organization of the adsorbed layer is controlled by both surface topography and chemistry.[43] For the amphiphilic protein HPF, an environment-dependent conformation can be observed (*e.g.*, isoelectric point of buffer solution or surface chemistry).[41] In this study, on hydrophilic MD UHMWPE surfaces, the effect of surface morphology on HPF adsorption is strongly reduced or even absent compared to hydrophobic MD UHMWPE, as a systematic orientation of adsorbed HPF molecules with respect to the surface topography like, for example, the lamellar structure cannot be resolved.

Summary. From the assembly and orientation of adsorbed HPF, we obtained information on the influence of the surface nanostructure on protein−surface and protein−protein interactions. As such, MD UHMWPE surfaces are ideally suited to study protein interactions by AFM on polymeric implants at molecular resolution.

In contrast to previous studies,[35,40,44] we observed for the first time to our knowledge that the surface topography can influence the protein aggregation and induce a nonrandom network structure. Crystalline regions may trigger a favored assembly of HPF by local differences in surface free energy between the crystalline lamellae and the amorphous regions, which is neutralized on a hydrophilic surface. This insight could also be relevant for the ongoing discussion on local driving forces for protein−surface and protein−protein interactions and thereupon cellular response on nanostructured biomedical surfaces, such as created by amphiphilic block copolymers.[45] Future experiments need to address the influence of polymer nanostructure-induced protein assembly on the biological functionality, such as the cross-linking and blood coagulation capability, fibrinolysis, and cellular interactions for HPF.[46]

CONCLUSION

The current study shows how surface nanotopography, surface chemistry, and crystallinity influence the assembly and orientation of HPF onto UHMWPE surfaces.

On hydrophobic UHMWPE, the surface nanotopography partially aligns single HPF molecules with their trinodular axis parallel to the crystalline lamellae and induces anisotropic ringlike network structures. At close to monolayer coverage, it suppresses these ringlike networks. In contrast, on UHMWPE surfaces which are smooth on the nanoscale, the star-like assembly and the undisturbed ring network of HPF indicate increased surface diffusion and enhanced protein−protein interactions in the absence of nanotopography. Furthermore, the nanotopography does not induce any HPF alignment on hydrophilic UHMWPE surfaces ascribed to dominating protein−surface interactions.

The approach to exploit molecularly self-assembled, nanostructured surfaces as described in this work permits insight into the biological response to biomaterials' surfaces on the molecular and supramolecular scale. It further enlightens strategies to create oriented protein nanopatterns on polymer surfaces to optimize surface functionalities, such as lubrication properties of UHMWPE in endoprosthetic devices.

METHODS

MD UHMWPE Film Generation. Ultraflat, highly oriented MD UHMWPE thin films were produced by the melt drawn technique described as follows: UHMWPE powder (Sigma Aldrich, Schnelldorf, Germany, molecular weight $M_w = 3 \times 10^6$ to 6×10^6 g/mol) was dissolved in xylene (synthesis grade, Merck KGaA, Darmstadt, Germany) at a concentration of 0.1 wt % and heated to ~120 °C. The UHMWPE solution was poured onto a glass slide mounted on a heating plate kept at a temperature of ~140 °C. After evaporation of the solvent, a thin UHMWPE film was drawn from the polymer melt (Figure 1) at a drawing rate of ~1 cm/s by tweezers.[19] The originally free-standing film was fixed on a glass slide covered with a Au layer to improve the film stability. To render the MD UHMWPE surfaces hydrophilic, an argon plasma (PDC-32G, Harrick Plasma, New York, USA, radio frequency of 8−12 MHz, power of 10.5 W) was applied for a period of 60 s at a pressure of 0.25 mbar.

AFM Analysis. AFM topographic images of the native or plasma-treated UHMWPE surfaces before and after protein adsorption were recorded in tapping mode at a scan rate of 2 Hz. A Dimension 3100 AFM (Digital Instruments, Veeco, Santa Barbara, CA, USA) with a Nanoscope IV controller at ambient temperature in air and standard tapping mode silicon cantilevers (Olympus OMCL-AC160TS, Atomic Force F&E GmbH,

Mannheim, Germany) with a typical resonance frequency of 300 kHz and a cantilever stiffness of 42 N/m were used. A first-order flattening function was applied to the AFM micrographs. To emphasize the adsorbed proteins on the UHMWPE film, a local balancing image analysis routine (Corel-Photo Paint X3) followed by a contrast enhancement was globally applied to AFM gray scale images. A quantitative analysis of the total amount of adsorbed protein is not possible, as AFM provides only local information and the adsorption into multiple protein layers at higher concentrations restricts the quantification solely based on surface coverage values. We therefore did not attempt to determine the total amount of adsorbed protein, which is subject to future work.

ToF-SIMS, XPS, and Contact Angle Analysis. Time-of-flight secondary-ion mass spectrometry (ToF-SIMS) high-resolution mass spectra were acquired with a reflector-type spectrometer (ION-TOF TOFSIMS IV), by using a pulsed $^{69}Ga^{+}$ primary ion beam (25 keV, ~0.1 pA).[47] Complementary, the surface modification of the UHMWPE films was analyzed by X-ray photoelectron spectroscopy (XPS). High-resolution spectra were recorded with a Quantum 2000 (PHI Co., Chanhassen, MN, USA) apparatus with a focused monochromatic Al Kα source (1486.7 eV) for excitation. The pass energy was 23.5 eV. The water contact angle was determined from the shape of axisymmetric menisci of sessile distilled water drops using a DSA10 drop shape analysis system (Kruss GmbH, Hamburg, Germany).

Protein Adsorption. A stock solution of HPF (Calbiochem, Merck KGaA, Darmstadt, Germany) in phosphate buffered saline solution (PBS) was prepared with a HPF concentration of 200 mg/L. For concentration-dependent adsorption studies, the stock solution was diluted with PBS to concentrations of 1−10 mg/L. For each concentration, 1 mL was pipetted on the native or plasma-treated MD UHMWPE films and left for adsorption for 2 h under quasi-physiological conditions at 37 °C and pH 7.4 to reach equilibrium.[35,39] Then, the samples were rinsed twice with PBS to prevent further adsorption from the buffer solution. Subsequently, they were rinsed with distilled water to remove not adsorbed proteins and PBS residues and finally dried in compressed air.

Acknowledgment. We thank Mr. Ralf Wagner, Institute of Material Science and Technology (IMT), FSU, for conducting the XPS measurements. We gratefully acknowledge the partial support from the German Academic Exchange Service (DAAD) through the Italian−German exchange program VIGONI, project number D/07/15305, and from the BMBF within the project Innovations- und Gründerlabor für neue Werkstoffe und Verfahren (IGWV) an der Friedrich-Schiller-Universität Jena, Förderkennzeichen: 03GL0026.

REFERENCES AND NOTES

1. Lord, M. S.; Foss, M.; Besenbacher, F. Influence of Nanoscale Surface Topography on Protein Adsorption and Cellular Response. *Nano Today* **2010,** *5*, 66–78.
2. Scopelliti, P. E.; Borgonovo, A.; Indrieri, M.; Giorgetti, L.; Bongiorno, G.; Carbone, R.; Podesta, A.; Milani, P. The Effect of Surface Nanometre-Scale Morphology on Protein Adsorption. *PLoS One* **2010,** 5.
3. Chen, H.; Yuan, L.; Song, W.; Wu, Z. K.; Li, D. Biocompatible Polymer Materials: Role of Protein−Surface Interactions. *Prog. Polym. Sci.* **2008,** *33*, 1059–1087.
4. Granchi, D.; Ciapetti, G.; Amato, I.; Pagani, S.; Cenni, E.; Savarino, L.; Avnet, S.; Peris, J. L.; Pellacani, A.; Baldini, N.;*et al.*The Influence of Alumina and Ultra-High Molecular Weight Polyethylene Particles on Osteoblast−Osteoclast Cooperation. *Biomaterials* **2004,** *25*, 4037–4045.
5. Gonzalez-Mora, V. A.; Hoffmann, M.; Stroosnijder, R.; Gil, F. J. Wear Tests in a Hip Joint Simulator of Different CoCrMo Counterfaces on UHMWPE. *Mater. Sci. Eng. C* **2009,** *29*, 153–158.
6. Ren, W. P.; Markel, D. C.; Zhang, R.; Peng, X.; Wu, B.; Monica, H.; Wooley, P. H. Association between UHMWPE Particle-Induced Inflammatory Osteoclastogenesis and Expression of RANKL, VEGF, and Flt-1 *In Vivo*. *Biomaterials* **2006,** *27*, 5161–5169.
7. Heuberger, M. P.; Widmer, M. R.; Zobeley, E.; Glockshuber, R.; Spencer, N. D. Protein-Mediated Boundary Lubrication in Arthroplasty. *Biomaterials* **2005,** *26*, 1165–1173.
8. Berglin, M.; Pinori, E.; Sellborn, A.; Andersson, M.; Hulander, M.; Elwing, H. Fibrinogen Adsorption and Conformational Change on Model Polymers: Novel Aspects of Mutual Molecular Rearrangement. *Langmuir* **2009,** *25*, 5602–5608.
9. Dolatshahi-Pirouz, A.; Jensen, T.; Kraft, D. C.; Foss, M.; Kingshott, P.; Hansen, J. L.; Larsen, A. N.; Chevallier, J.; Besenbacher, F. Fibronectin Adsorption, Cell Adhesion, and Proliferation on Nanostructured Tantalum Surfaces. *ACS Nano* **2010,** *4*, 2874–2882.
10. Messina, G. M. L.; Satriano, C.; Marletta, G. Confined Protein Adsorption into Nanopore Arrays Fabricated by Colloidal-Assisted Polymer Patterning. *Chem. Commun.* **2008,** 5031–5033.
11. Parhi, P.; Golas, A.; Barnthip, N.; Noh, H.; Vogler, E. A. Volumetric Interpretation of Protein Adsorption: Capacity Scaling with Adsorbate Molecular Weight and Adsorbent Surface Energy. *Biomaterials* **2009,** *30*, 6814–6824.
12. Karuppiah, K. S. K.; Bruck, A. L.; Sundararajan, S.; Wang, J.; Lin, Z. Q.; Xu, Z. H.; Li, X. D. Friction and Wear Behavior of Ultra-High Molecular Weight Polyethylene as a Function of Polymer Crystallinity. *Acta Biomater.* **2008,** *4*, 1401–1410.
13. Keller, T. F.; Müller, M.; Ouyang, W.; Zhang, J. T.; Jandt, K. D. Templating α-Helical Poly(L-lysine)/Polyanion Complexes by Nanostructured Uniaxially Oriented Ultrathin Polyethylene Films. *Langmuir* **2010,** *26*, 18893–18901.
14. Ohta, M.; Hyon, S. H.; Kang, Y. B.; Oka, M.; Tsutsumi, S.; Murakami, S.; Kohjiya, S. Wear Properties of UHMWPE Oriented under Uniaxial Compression During the Molten State and at Lower Temperatures Than the Melting Point. *JSME Int. J. C* **2003,** *46*, 1297–1303.
15. Wirtz, D. C.; Schopphoff, E.; Weichert, D.; Niethard, F. U. Stretched Polyethylene (UHMWPE)—A New Material Modification That Reduces Wear in Total Knee Arthroplasty. *Biomed. Tech.* **2001,** *46*, 338–342.
16. Chang, N.; Bellare, A.; Cohen, R. E.; Spector, M. Wear Behavior of Bulk Oriented and Fiber Reinforced UHMWPE. *Wear* **2000,** *241*, 109–117.
17. Jandt, K. D. Atomic Force Microscopy of Biomaterials Surfaces and Interfaces. *Surf. Sci.* **2001,** *491*, 303–332.
18. Holland, N. B.; Marchant, R. E. Individual Plasma Proteins Detected on Rough Biomaterials by Phase Imaging AFM. *J. Biomed. Mater. Res.* **2000,** *51*, 307–315.
19. Keller, T.; Grosch, M.; Jandt, K. D. Nanoscale Surface Lamellar Orientation and Lamellar Doubling in Ultrathin UHMW-PE Films. *Macromolecules* **2007,** *40*, 5812–5819.
20. Petermann, J.; Gohil, R. M. New Method for the Preparation of High Modulus Thermoplastic Films. *J. Mater. Sci.* **1979,** *14*, 2260–2264.
21. Jandt, K. D.; Mc Master, J.; Miles, M. J.; Petermann, J. Scanning Force Microscopy of Melt-Crystallized, Metal-Evaporated Poly-(butene-1) Ultra-Thin Films. *Macromolecules* **1993,** *26*, 6552–6556.
22. Jandt, K. D.; Buhk, M.; Miles, M. J.; Petermann, J. Shish-Kebab Crystals in Polyethylene Investigated by Scanning Force Microscopy. *Polymer* **1994,** *35*, 2458–2462.
23. Keller, T.; Semmler, C.; Jandt, K. D. Strain-Induced Phase Morphology in Melt Drawn Ultrathin Highly Oriented Block Copolymer Films. *Macromol. Rapid Commun.* **2008,** *29*, 876–884.
24. Scott, E. A.; Elbert, D. L. Mass Spectrometric Mapping of Fibrinogen Conformations at Poly(ethylene terephthalate) Interfaces. *Biomaterials* **2007,** *28*, 3904–3917.
25. Hao, J. Y.; Keller, T.; Cai, K.; Klemm, E.; Bossert, J.; Jandt, K. D. The Effect of D,L-Lactidyl/ε-Caproyl Weight Ratio and Chemical Microstructure on Surface Properties of Biodegradable Poly(D,L-lactide)-*co*-Poly(ε-Caprolactone) Random Copolymers. *Adv. Eng. Mater.* **2008,** *10*, B23–B32.
26. Gobezie, R.; Kho, A.; Krastins, B.; Sarracino, D. A.; Thornhill, T. S.; Chase, M.; Millett, P. J.; Lee, D. M. High Abundance Synovial Fluid Proteome: Distinct Profiles in Health and Osteoarthritis. *Arthritis Res. Ther.* **2007,** 9.

27. Gibson, D. S.; Rooney, M. E. The Human Synovial Fluid Proteome: A Key Factor in the Pathology of Joint Disease. *Proteomics Clin. Appl.* **2007,** *1*, 889–899.
28. Kummer, J. A.; Abbink, J. J.; Deboer, J. P.; Roem, D.; Nieuwenhuys, E. J.; Kamp, A. M.; Swaak, T. J. G.; Hack, C. E. Analysis of Intraarticular Fibrinolytic Pathways in Patients with Inflammatory and Noninflammatory Joint Diseases. *Arthritis Rheum.* **1992,** *35*, 884–893.
29. Jandt, K. D.; Buhk, M.; Petermann, J. Microscopic Aspects of Polymer−Metal Epitaxy. *J. Mater. Sci.* **1996,** *31*, 1779–1788.
30. Ta, T. C.; Sykes, M. T.; McDermott, M. T. Real-Time Observation of Plasma Protein Film Formation on Well-Defined Surfaces with Scanning Force Microscopy. *Langmuir* **1998,** *14*, 2435–2443.
31. Svorcik, V.; Kotal, V.; Siegel, J.; Sajdl, P.; Mackova, A.; Hnatowicz, V. Ablation and Water Etching of Poly(ethylene) Modified by Argon Plasma. *Polym. Degrad. Stab.* **2007,** *92*, 1645–1649.
32. Xu, L. C.; Siedlecki, C. A. Effects of Surface Wettability and Contact Time on Protein Adhesion to Biomaterial Surfaces. *Biomaterials* **2007,** *28*, 3273–3283.
33. Sit, P. S.; Marchant, R. E. Surface-Dependent Conformations of Human Fibrinogen Observed by Atomic Force Microscopy under Aqueous Conditions. *Thromb. Haemostasis* **1999,** *82*, 1053–1060.
34. Cacciafesta, P.; Humphris, A. D. L.; Jandt, K. D.; Miles, M. J. Human Plasma Fibrinogen Adsorption on Ultraflat Titanium Oxide Surfaces Studied with Atomic Force Microscopy. *Langmuir* **2000,** *16*, 8167–8175.
35. Gettens, R. T. T.; Bai, Z. J.; Gilbert, J. L. Quantification of the Kinetics and Thermodynamics of Protein Adsorption Using Atomic Force Microscopy. *J. Biomed. Mater. Res. A* **2005,** *72A*, 246–257.
36. Reichert, J.; Wei, G.; Jandt, K. D. Formation and Topotactical Orientation of Fibrinogen Nanofibrils on Graphite Nanostructures. *Adv. Eng. Mater.* **2009,** *11*, B177–B181.
37. Marchin, K. L.; Berrie, C. L. Conformational Changes in the Plasma Protein Fibrinogen upon Adsorption to Graphite and Mica Investigated by Atomic Force Microscopy. *Langmuir* **2003,** *19*, 9883–9888.
38. Karuppiah, K. S. K.; Sundararajan, S.; Xu, Z. H.; Li, X. D. The Effect of Protein Adsorption on the Friction Behavior of Ultra-High Molecular Weight Polyethylene. *Tribol. Lett.* **2006,** *22*, 181–188.
39. Roach, P.; Farrar, D.; Perry, C. C. Interpretation of Protein Adsorption: Surface-Induced Conformational Changes. *J. Am. Chem. Soc.* **2005,** *127*, 8168–8173.
40. De Keere, I. V.; Willaert, R.; Hubin, A.; Vereeckent, J. Interaction of Human Plasma Fibrinogen with Commercially Pure Titanium As Studied with Atomic Force Microscopy and X-ray Photoelectron Spectroscopy. *Langmuir* **2008,** *24*, 1844–1852.
41. Tunc, S.; Maitz, M. F.; Steiner, G.; Vazquez, L.; Pham, M. T.; Salzer, R. *In Situ* Conformational Analysis of Fibrinogen Adsorbed on Si Surfaces. *Colloids Surf. B* **2005,** *42*, 219–225.
42. Steiner, G.; Tunc, S.; Maitz, M.; Salzer, R. Conformational Changes during Protein Adsorption. FT-IR Spectroscopic Imaging of Adsorbed Fibrinogen Layers. *Anal. Chem.* **2007,** *79*, 1311–1316.
43. Denis, F. A.; Hanarp, P.; Sutherland, D. S.; Gold, J.; Mustin, C.; Rouxhet, P. G.; Dufrene, Y. F. Protein Adsorption on Model Surfaces with Controlled Nanotopography and Chemistry. *Langmuir* **2002,** *18*, 819–828.
44. Lin, Y.; Wang, J.; Wan, L. J.; Fang, X. H. Study of Fibrinogen Adsorption on Self-Assembled Monolayers on Au(111) by Atomic Force Microscopy. *Ultramicroscopy* **2005,** *105*, 129–136.
45. Matsusaki, M.; Omichi, M.; Kadowaki, K.; Kim, B. H.; Kim, S. O.; Maruyama, I.; Akashi, M. Protein Nanoarrays on a Highly-Oriented Lamellar Surface. *Chem. Commun.* **2010,** *46*, 1911–1913.
46. Mosesson, M. W. Fibrinogen and Fibrin Structure and Functions. *J. Thromb. Haemostasis* **2005,** *3*, 1894–1904.
47. Tuccitto, N.; Giamblanco, N.; Marletta, G.; Licciardello, A. ToF-SIMS Investigation of FIB-Patterning of Lactoferrin by Using Self-Assembled Monolayers of Iron Complexes. *Appl. Surf. Sci.* **2008,** *255*, 1075–1078.